Original article

A Computational Study: Structural and Electronic Properties of Some Transition Metal Doped Bilayer Graphene Systems

Özlem Ünlü [iD] [a, *] & İzzet Amour Morkan [iD] [b]

[a] Department of Chemistry, Faculty of Arts and Science, Duzce University, Duzce, Turkey
[b] Department of Chemistry, Faculty of Arts and Science, Bolu Abant İzzet Baysal University, Bolu, Turkey

Abstract

Graphene, which is accepted as the main material of nanomaterials, attracts great attention thanks to its applicability in almost every field and its superior properties. The zero-band graphene gap is a problem that scientists must overcome in designing new electronics. Tailoring the electronic properties of graphene systems by making a change in the band gap allow us great advantages. In this study, Intercalation of transition metal (TM) atom to graphene systems as sandwich-like graphene|TM|graphene structures were investigated by ab initio first principle Density Functional Theory (DFT) computations. GGA with BPW91 basis set were used for DFT calculations. DFT calculations were performed on W, Re, and Os transition metal atoms intercalted between bilayer graphene (BLG). After geometry optimization of graphene|TM|graphene structures, graphene layers doped with nitrogen atoms by substitutional doping for investigation of change in electronic behavior. The electronic behaviour of metal intercalated BLG structures can be modified by type of transition metal and dopant as a result of charge transfer. Substitutional doping with nitrogen atoms to graphene structures showed a change in local density due to the charge transfer as a result of its extra one electron. Placing a transition metal atom between BLG layers leads to constriction in the band gap with a boost in conductive character.

Keywords: Graphene|TM|graphene , band gap opening, bilayer graphene systems, DFT.

---

[*] **Corresponding author:**

Özlem Ünlü is a Research Assistant Dr. in the Department of Chemistry at Düzce University in Düzce, Turkey. Her research interests include the Chemistry, Inorganic Chemistry, Theoretical Chemistry and Nanomaterials. Submitted manuscript was produced from her doctoral thesis. She studied in Bolu Abant İzzet Baysal University in Bolu, and worked in Düzce University in Düzce, Turkey.
Email: ozlemilkin@duzce.edu.tr

INTRODUCTION

Graphene is an allotrope of carbon atoms in the form of a hexagonal honeycomb lattice in two-dimension. Graphene and graphite are composed of pure sp^2 hybrid carbon atoms and have similar physical properties. These general structural properties indicate that graphene is the fundamental structural molecule of all graphitic carbon structures; fullerenes, carbon nanotubes, graphite. (Randviir, Brownson, & Banks, 2014; Zhen & Zhu, 2018). Graphene research has generated enormous interest in the scientific community since its original discovery by Geim and Novoselov in 2004 (Novoselov et al., 2004, 2005). As the "mother" of nanomaterials, graphene has outstanding unique properties; it has the high electrical and thermal conductivity, elasticity, flexibility, hardness, and resistance (Georgakilas et al., 2012; Hu, Yao, & Wang, 2017; Naumis, Barraza-Lopez, Oliva-Leyva, & Terrones, 2017). Over the decades, increased number of research regarding to applications of graphene has increased its potential for applications in energy storage, environmental solutions, and medicinal technologies (Allen, 2009; Randviir et al., 2014; Wang, Sun, Tao, Stacchiola, & Hu, 2013; Zhao, Hayner, Kung, & Kung, 2011).

The bilayer graphene (BLG) structure can exist in AA, AB or twisted bilayer modifications. The most stable configuration is graphite-like layer which is the AB modification of BLG (Rozhkov, Sboychakov, Rakhmanov, & Nori, 2016). BLG shows similar properties with monolayer graphene (MLG)(Mccann & Koshino, 2013) however it differs from MLG by its low energy band structure. They both have zero band gap between their conduction and valence bands. The charge carriers in MLG is linear in MLG with massless chiral quasiparticles as described in Dirac-like effective Hamiltonian (Castro Neto, Guinea, Peres, Novoselov, & Geim, 2009) whereas in BLG, the dispersion is quadratic with massive chiral quasiparticles(Mccann & Koshino, 2013; Rozhkov et al., 2016). The low-energy BLG Hamiltonian can be seen as a principle of the Dirac Hamiltonian of single-layer graphene, which leads to a more complex structure of the scattering of electrons and holes. Tuning the physical properties by making a change in the band gap of BLG allows us great advantages. There are several mechanisms for opening a band gap in BLG systems with applying an electrical field or molecular doping. Theoretical studies reveal that applying an external electric field produces a tunable band gap (Hao et al., 2015; Zhang et al., 2011). Another way is chemical doping which leads us to modify materials by tailoring electronic properties, generation of local changes in the elemental composition of main materials, and manipulating surface chemistry. In addition, chemical doping also gives the advantage of controlling the enrichment of free charge-carrier density and enhancing the electrical or thermal conductivity(Guo & Dong, 2011). As neighbors of carbon, boron and nitrogen are studied as dopants in carbon chemistry with minimal difference in covalent radii (Luo et al., n.d.; Tison et al., 2015). Studies have shown that doping with B or N can modulate the band structure of carbon-based systems (Kuroki et al., 2008). Intercalation of transition metal chromium atom to graphene systems as sandwich-like graphene|metal|ligand structure was theoretically studied, and it is concluded

that the π-3d interactions result in a change in band structure (Avdoshenko, Ioffe, Cuniberti, Dunsch, & Popov, 2011; Bui, Le, Kawazoe, & Nguyen-Manh, 2013; Miramontes et al., 2015). In this article, *ab initio* first-principles DFT computations were performed to investigate the electronic behaviour of BLG systems with substitutional doping of nitrogen, and intercalation of certain atoms rare transition metals between graphene layers for further experimental studies on new electronics and nanocatalyst synthesis.

COMPUTATIONAL DETAILS

In this study, the Atomistic-ToolKit 2017.2 Synopsys Quantum Wise A/S (Atomistix Toolkit version 2017.2, 2017) software is used to carry out *ab initio* first-principles DFT calculations for transition metals of rhenium, tungsten, osmium intercalated graphene|TM|graphene systems. Generalized gradient approximation (GGA) is used for first-principles DFT calculations. Becke exchange combined with Perdew-Wang-91 (BPW91) basis set is chosen for DFT. Linear combination of atomic orbitals (LCAO) calculator is used for computations.

RESULTS and DISCUSSION

Structures and Geometry Optimizations

In the first step, geometry optimizations were accomplished for detailed DFT calculations. The optimization calculations were performed for all eight graphene-based structures. The abbreviations of these structures were coded by their initial letters; monolayer graphene; MLG, bilayer graphene; BLG, metal intercalated bilayer graphene; MBLG, for metals of rhenium, tungsten and osmium; ReBLG, WBLG, OsBLG, and nitrogen doped metal intercaleted bilayer graphene for metals of rhenium, tungsten and osmium; ReNBLG, WNBLG, OsBLG.

Bilayer graphene structure was generated from graphite. After AB stacking BLG was built transition metal atoms were intercalated between graphene layers. Optimized of geometries for presented structures with various number of carbon atoms were computed. Calculations of bond lengths between carbon-carbon (C-C), metal-carbon (M-C), nitrogen-carbon (N-C), and oxygen-carbon (O-C) atoms in the structures were shown in Table 1.

Table 1. Bond lengths between certain atoms in geometrically optimized graphene-based structures

	C-C	M-C	N-C	O-C	Layer Distance
MLG	1.43				
BLG (2X2)	1.42				4.64
BLG (4X4)	1.44				4.36
ReBLG	1.43	2.37			4.25
WBLG	1.47	2.13			4.26
OsBLG	1.41	2.11			4.28
ReNBLG	1.43	2.15	1.44		4.37
WNBLG	1.44	2.17	1.44		4.32
OsNBLG	1.44	2.18	1.44		4.21

The optimized geometries of each studied structure are as shown in Figure 1. Structural optimization data showed that in the structure each one with symmetry of C_1[1].
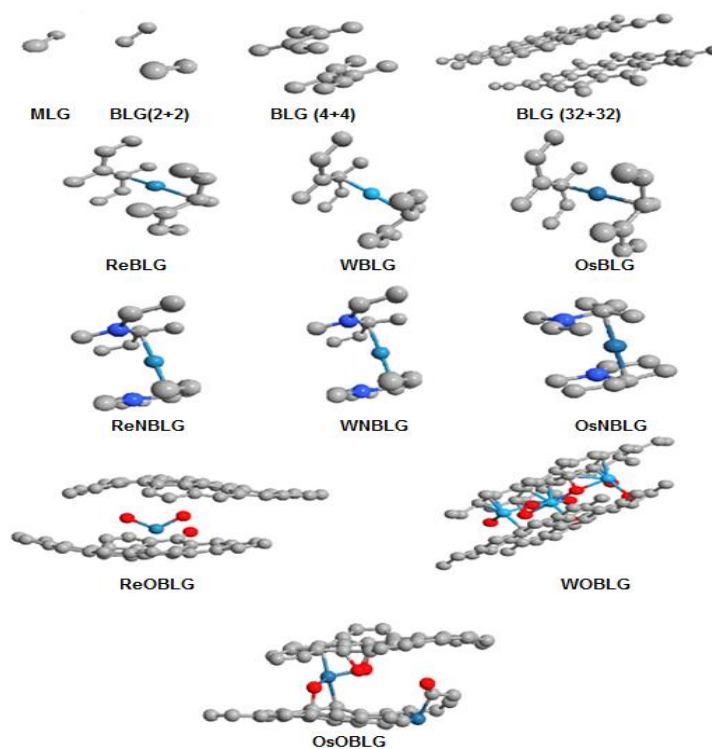
Figure 1 Optimized geometries of graphene structures; carbon atoms represented in grey, metal atoms (M: Re, W, Os) represented in blue, nitrogen atoms represented in purple, and oxygen atoms represented in red.

The bond lengths of graphene|TM|graphene structures (TM; Re, W, Os) were calculated for both raw and optimized geometries, and it was found that the metal insertion caused an expansion of the distance between the graphene layers. Even though metal insertion between the graphene layers does not significantly affect the C-C bond, nitrogen doping causes the distance between the layers to increase.

The energy term data are given in Table 2 for the predicted graphene structures. The combined energies of thestructures revealed that BLG has fewer free energy than MLG, which means that adding layers to the graphene structure becomes more stable. Also the insertion of metal to BLG caused an increase in energy in all respects, however, the insertion of metal oxides in the two-layer graphene reduced the total free energy.

Table 2. The total energies of MGL, BGL, WBLG, ReBLG, OsBLG, MBLG (M; W, Re, Os)

	Exchange-Correlation	Kinetic Energy	Electrostatic Energy	Entropy-Term	Total free energy
MLG	-900.9	2064.6	-3987.6	-0.12	-2824.05
BLG	-769.3	1709.9	-3413.2	-0.16	-2472.62
WBLG	-1105.6	1950.7	-3777.8	-0.04	-2932.83
ReBLG	-1007.8	2022.1	-3925.3	-0.03	-2911.13
OsBLG	-1041.8	2103.1	-4102.1	-0.02	-3040.68
MNBLG	-1284.6	1908.1	-3951.5	-0.04	-3329.00

Graphs of the angular and radial distribution of graphene systems are shown in Figure 2. The angular distribution of the MLG shows only one peak at 120°, while radial distribution of MLG structure shows three relative peaks due to the configurations of carbon atoms in the sp2 hybridized honeycomb lattice. On the contrary, BLG exhibits many inhomogeneous peaks due to the Bernard configuration. When a metal atom was sandwiched between graphene-carbon-metal layers, it exhibited higher angular/radial distributions than carbon-carbon atoms; however, as expected, the highest distribution was calculated for the MNBLG structures.
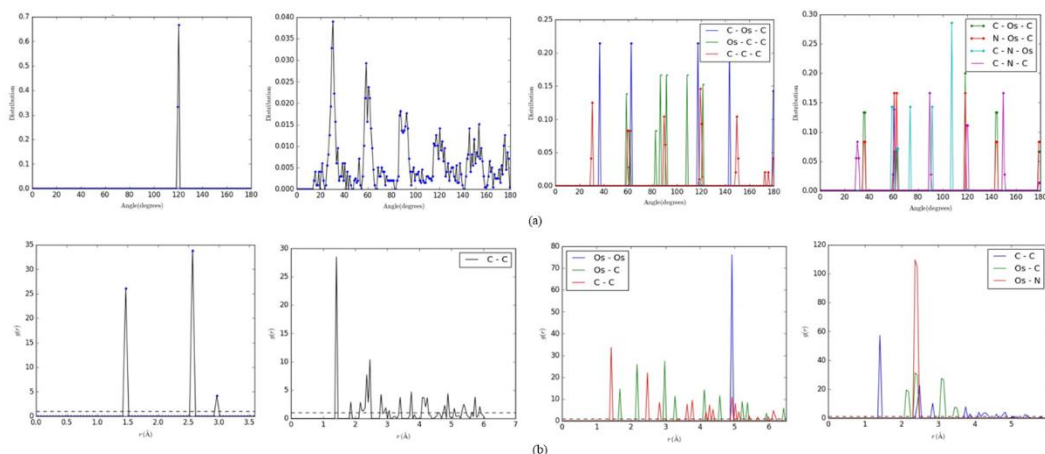

Figure 2. a) Angular distribution of MLG, BLG, OsBLG, OsNBLG, **b)** Radial distribution of MLG, BLG, OsBLG, OsNBLG

Band Structure Analysis

Band structure analyses were investigated using *ab initio* pseudopotential approach with exchange-correlation, GGA formalism in Becke's exchange combined with Perdew Wang basis set (BPW91) after structure relaxation to modify and control the properties electronics of these compounds to provide electrocatalytic mechanisms to produce useful material. Band structures of the optimized graphene systems were given in Figure 3. The MLG shows a zero band gap at point K. To open the bandgap in BLG, an electric field is first applied, moving the first metallic domain to 0 V and the second

to 10 V to change their size so that they cover the hexagonal unit cell entirely. Applied voltage gives 4 V/nm in z direction which is slightly above the field that was found in band-gap tailoring experiments. The theoretical lattice constant for BLG was 2.4612 Å, the calculated bandgap was 1.1682 eV at the Fermi level. The WBLG band gap was 0.04617 eV, the ReBLG band gap was 0.086524 eV, and the OsBLG band gap was 0.11472 eV. Band structure analysis showed that MNBLG structures showed in a small opening in band gap with WNBLG band gap of 0.076143 eV at Fermi level. Data shows us doped nitrogen and insertion of transition metal result in narrowing the band gap while rises the conductor behaviour of structures. Band-gap analysis showed that MNBLG structures result in a small bandgap opening, with a WNBLG bandgap of 0.076143 eV at the Fermi level. The data show that doped nitrogen and the introduction of transition metal atom leads to a narrowing of the band gap, while the conductor nature of the structures increases.
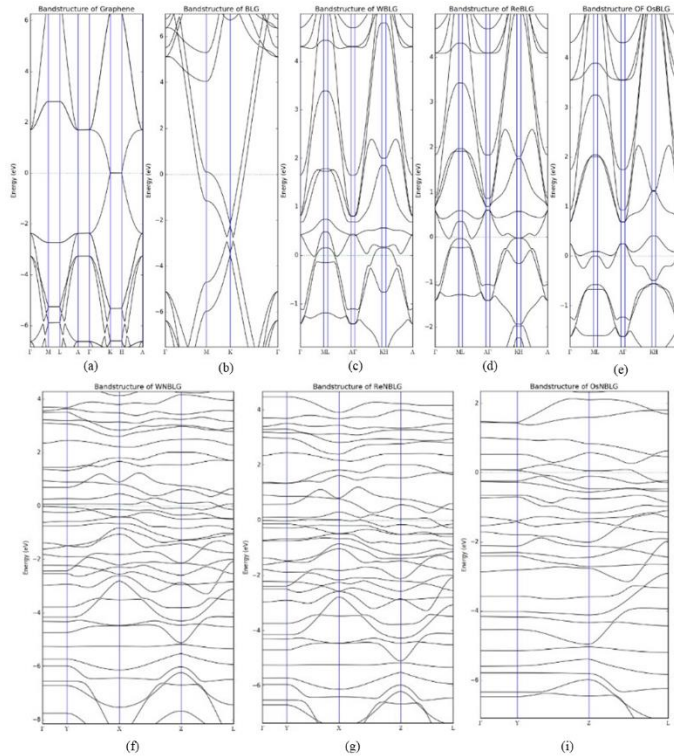
Figure 3. Band structures a) MLG, b) BLG, c) WBLG, d) ReBLG, e) OsBLG, f) WNBLG, g) ReNBLG, i) OsNBLG.

The effective hole and electron mass that fitted the parabola to the min/max of the conduction band/valence band was calculated for lattice structures for different band indices and is given in Table 3.

Table 3. The effective hole and mass of conduction/valance bands

|	Band Index	Energy (eV)	m* (mₑ)
MLG	4	-13.403	0.233
	5	-13.403	0.088
BLG	4	-15.765	0.062
	5	-14.158	0.648
WBLG	0	-19.663	1.440
	1	-19.514	1.448
ReBLG	0	-20.324	1.442
	1	-20.138	1.448
WNBLG	0	-22.416	2.010
	1	-22.248	2.200
ReNBLG	4	-23.538	-0.426
	5	-20.619	11.369
OsNBLG	4	-23.274	-102.963
	5	-20.401	18.810

Electronic property analysis

Analysis of the electron density of each structure, calculated and modeled with the electron density analyzer in ATK. Isosurfaces and 3D cross-sectional models for each structure are shown in Figure 4a, b. One-dimensional graphical projections were exported from ATK electron density analysis for the sum of the up and down rotational projections along the a, b, and c axes with a unit of 1/Angs3 as shown in Figure 4c.
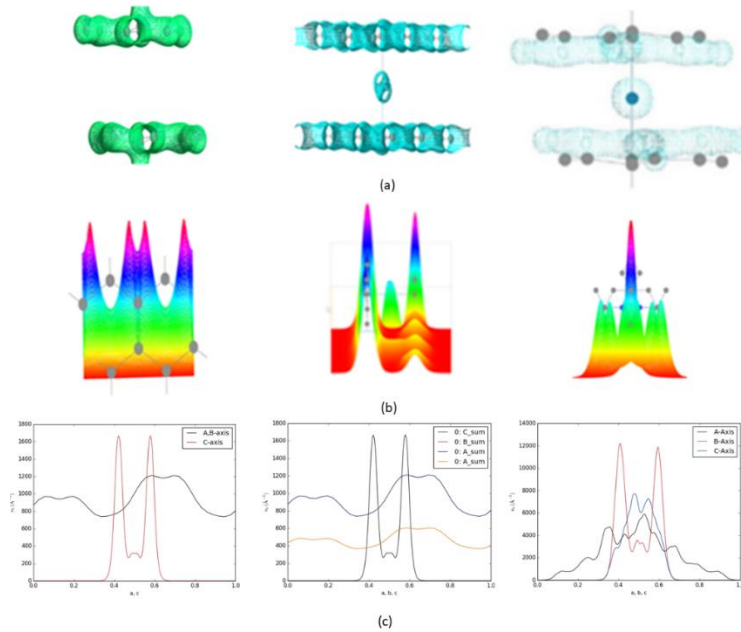
Figure 4. Electron density scheme of BLG, MBLG, MNBLG a) isosurface, b) three-dimensional cross-section plane models, c) one-dimensional projection plot

The electron density diagrams of the bilayer structure of graphene in the isosurface and three-dimensional section plane models showed a uniform distribution, since only carbon atoms were present in the Bernal stack. After the transition metals were introduced into the midpoint of the two-layer graphene, a significant change in electron density occurred. Nitrogen doping also caused a change in electron density.

Diagrams of electron difference densities of graphene structures were given in Figure 5. MNBLG showed unequal distribution of charge difference whereas MBLG has even allocation of electron difference density that transition metal atom and TM bonded carbon atoms have higher difference. Electron difference density diagrams of graphene structures are shown in Figure 5. MNBLG showed uneven charge difference distribution, while metal-insert bilayer graphene showed equal electron density difference distribution, with carbon atoms bonded to the metal and metal showing a big difference.
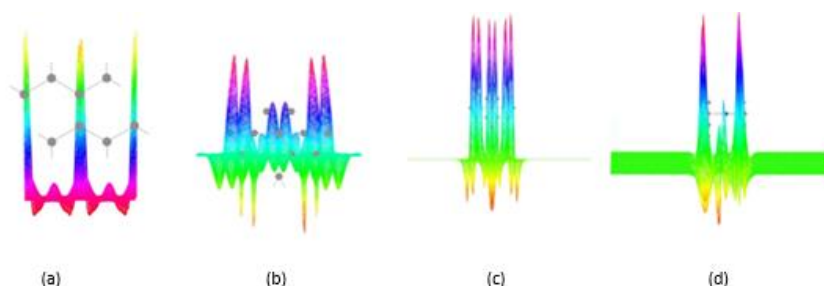

Figure 5. Electron difference density diagram (a) MLG, (b) BLG, (c) MBLG, (d) MNBLG

To explain the effect of atom changes on charge density, the partial charges within the structures sould be studied. Bader's analysis is a very effective method to study the effect of impurities and metallic inclusions on charge distribution. The complete Bader charge analysis is given in Figure 6. Bader's analysis showed that the charge distribution reveals a considerable change on carbon atoms adjacent to metal and nitrogen atoms. Thus, the overall charge maxima are balanced by a decrease in charge density on other sp^2 carbon atoms in the honeycomb structure. The topological charge density scheme is legitimate with respect to total free energiy and electron density. This means that the transition metal oxide intercalation is unpredictable. As a result, transition metal oxide clusters are not suitable for calculations.

An electron localization function (ELF) analysis of graphene|TM|graphene structures was calculated using first-principles DFT calculations and topological diagrams of WBLG and WNBLG with their molecular conformations are shown in Figure 7. The electron location function diagrams showed that the molecular distribution of electron pairs associated with the configurations, can be visualized from the ELF topological description.
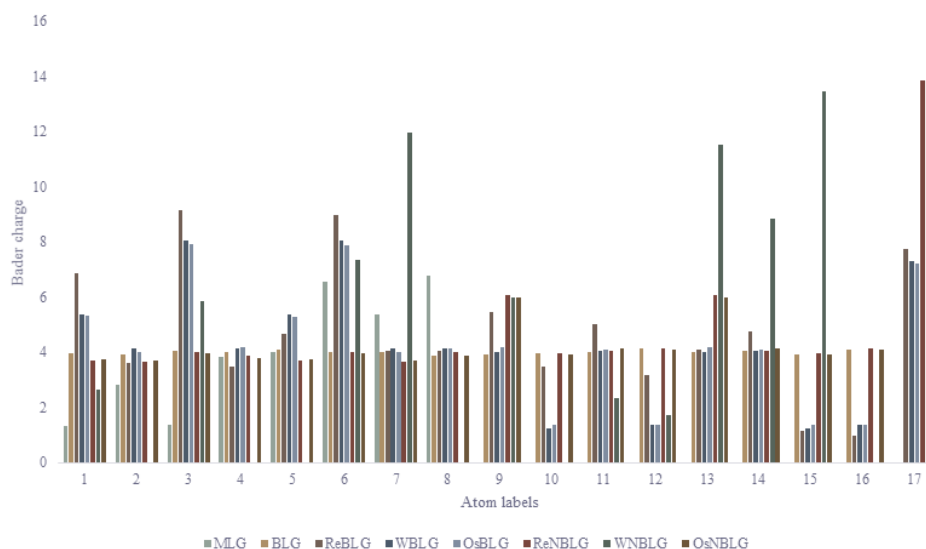
Figure 6. Bader analyses MLG,BLG, WBLG, ReBLG,OsBLG, WNBLG, OsNBLG
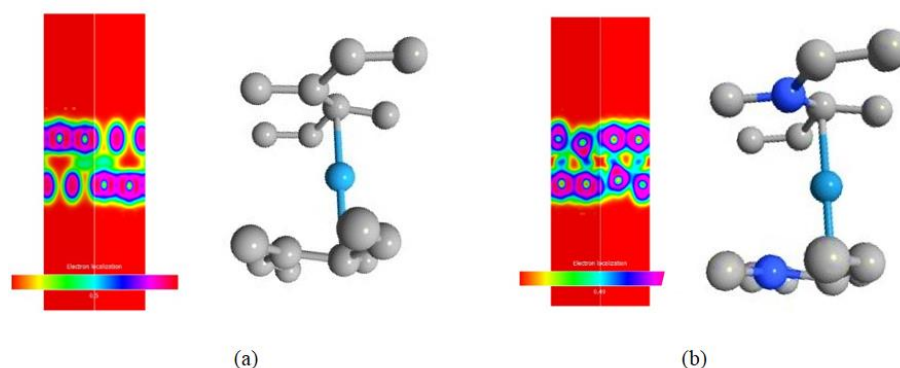
Figure 7. ELF models (a) MBLG, (b) MNBLG

Molecular energy analysis

Frontier Molecular Orbitals; HOMO and LUMO provide important computational chemistry parameters for π systems and electron transport mechanisms. For chemical stability, the energies of HOMO and LUMO must be evaluated, as well as the energy difference between these molecular orbitals. To determine the energies of HOMO/LUMO, TM intercalated BLG and nitrogen-doped MBLG molecular energy analyses were computed using exchange-correlation interactions by BPW91, DFT. The HOMO/LUMO energies of the structures are computed from the molecular energy spectra as shown in Table 4.

Table 4. HOMO/LUMO energies of the structures

	HOMO (eV)	LUMO (eV)
MLG	-3.087631	5.75000
BLG	-0.0142857	1.0002
ReBLG	-1.0009	0.60021
ReNBLG	-0.17857	0.35714

Conclusion

In this study, we presented first-principles *ab initio* DFT calculations to investigate the electronic character of BLG systems with insertion of some transition metal atoms (M: W, Re, Os) to BLG layers, doped with nitrogen atoms, and their electronic structure comparison with the MLG structure. The eight different graphene-based systems modeled based on lattice constant calculations of the graphite, and geometry optimizations were performed for achieving stable configurations. Behavior of electronic bands with change in structure, calculated using bandgap analysis. BLG shows zero bandgap at point K, an electric field was applied to open the bandgap by changing applied voltage of the second metal region, and then the cell size was adjusted to span the unit cell hexagonal. The utilized voltage was altered to 4 V/nm in the z-direction, that is slightly higher than the experimental data. The theoretical BLG lattice constant was found to be 2.4612 Å and the band gap at the Fermi level was 1.1682 eV. Band structure calculations for sandwich-like graphene|TM|graphene structures (TM; Re, W, Os) showed a band gap of 0.04617 eV, 0.086524 eV and 0.11472 eV, respectively. The nitrogen-doped WNBLG system at the Fermi level is calculated as 0.076143 eV. This shows us that modifications that match the band gap by intercalation of metal atoms into the graphene sheets improve conductivity. The each nanostructure was illuminated to understand electronic behaviour by means of electron density, electron difference density, and ELF analyses. Finally, a molecular orbital analysis was performed to determine the HOMO and LUMO energies.

The electronic behavior of sandwich-like graphene|TM|graphene structures (TM; Re, W, Os) can improve their electronic properties by being affected by the dopant atomand transition metal type. The calculated data presented in this study can be used for further experimental studies on new electronics and nanocatalyst synthesis, and guide experimental studies.

Acknowledgement

REFERENCES

Allen, M. (2009). Honeycomb carbon -- A study of graphene. *American Chemical Society*, 184.

Atomistix Toolkit version 2017.2, S. Q. A. (2017). *No Title*. Retrieved from www.quantumwise.com

Avdoshenko, S. M., Ioffe, I. N., Cuniberti, G., Dunsch, L., & Popov, A. A. (2011). Organometallic Complexes of Graphene: Toward Atomic Spintronics Using a Graphene Web. *ACS Nano*, *5*(12), 9939–9949.

Bui, V. Q., Le, H. M., Kawazoe, Y., & Nguyen-Manh, D. (2013). Graphene-Cr-graphene intercalation nanostructures: Stability and magnetic properties from density functional theory investigations. *Journal of Physical Chemistry C*, *117*(7), 3605–3614.

Castro Neto, A. H., Guinea, F., Peres, N. M. R., Novoselov, K. S., & Geim, A. K. (2009). The electronic properties of graphene. *Reviews of Modern Physics*, *81*(1), 109–162.

Georgakilas, V., Otyepka, M., Bourlinos, A. B., Chandra, V., Kim, N., Kemp, K. C., … Kim, K. S. (2012). Functionalization of graphene: Covalent and non-covalent approaches, derivatives and applications. *Chemical Reviews*, *112*(11), 6156–6214.

Guo, S., & Dong, S. (2011). Graphene and its derivative-based sensing materials for analytical devices. *Journal of Materials Chemistry*, *21*(46), 18503.

Hao, J., Huang, C., Wu, H., Qiu, Y., Gao, Q., Hu, Z., … Zhang, L. (2015). A promising way to open an energy gap in bilayer graphene. *Nanoscale*, *7*(40), 17096–17101.

Hu, M., Yao, Z., & Wang, X. (2017). Graphene-Based Nanomaterials for Catalysis. *Industrial and Engineering Chemistry Research*, *56*(13), 3477–3502.

Kuroki, K., Onari, S., Arita, R., Usui, H., Tanaka, Y., Kontani, H., & Aoki, H. (2008). Unconventional Pairing Originating from the Disconnected Fermi Surfaces of Superconducting LaFeAsO $1 - x$ F x. *Physical Review Letters*, *101*(8), 087004.

Luo, Z., Lim, S., Tian, Z., Shang, J., Lai, L., Macdonald, B., … Lin, J. (n.d.). *Pyridinic N doped graphene: synthesis, electronic structure, and electrocatalytic property*.

Mccann, E., & Koshino, M. (2013). *The electronic properties of bilayer graphene*.

Miramontes, O., Bonafé, F., Santiago, U., Larios-Rodriguez, E., Velázquez-Salazar, J. J., Mariscal, M. M., & Yacaman, M. J. (2015). Ultra-small rhenium clusters supported on graphene. *Physical Chemistry Chemical Physics*, *17*(12), 7898–7906.

Naumis, G. G., Barraza-Lopez, S., Oliva-Leyva, M., & Terrones, H. (2017). Electronic and optical properties of strained graphene and other strained 2D materials: A review. *Reports on Progress in Physics*, *80*(9), 096501.

Novoselov, K. S., Geim, A. K., Morozov, S. V, Jiang, D., Zhang, Y., Dubonos, S. V, … Firsov, A. A. (2004). Electric field effect in atomically thin carbon films. *Science (New York, N.Y.)*, *306*(5696), 666–669.

Novoselov, K. S., Jiang, D., Schedin, F., Booth, T. J., Khotkevich, V. V, Morozov, S. V, & Geim, A. K. (2005). Two-dimensional atomic crystals. *Proceedings of the National Academy of Sciences of the United States of America*, *102*(30), 10451–10453.

Randviir, E. P., Brownson, D. A. C., & Banks, C. E. (2014). A decade of graphene research: production, applications and outlook. *Materials Today*, *17*(9), 426–432.

Rozhkov, A. V., Sboychakov, A. O., Rakhmanov, A. L., & Nori, F. (2016). Electronic properties of graphene-based bilayer systems. *Physics Reports*, *648*, 1–104.

Tison, Y., Lagoute, J., Repain, V., Chacon, C., Girard, Y., Rousset, S., … Ducastelle, F. (2015). Electronic interaction between nitrogen atoms in doped graphene. *ACS Nano*, *9*(1), 670–678.

Wang, H., Sun, K., Tao, F., Stacchiola, D. J., & Hu, Y. H. (2013). 3D honeycomb-like structured graphene and its high efficiency as a counter-electrode catalyst for dye-sensitized solar cells. *Angewandte Chemie - International Edition*, *52*(35), 9210–9214.

Zhang, W., Lin, C.-T., Liu, K.-K., Tite, T., Su, C.-Y., Chang, C.-H., … Li, L.-J. (2011). Opening an Electrical Band Gap of Bilayer Graphene with Molecular Doping. *ACS Nano*, *5*(9), 7517–7524.

Zhao, X., Hayner, C. M., Kung, M. C., & Kung, H. H. (2011). In-plane vacancy-enabled high-power Si-graphene composite electrode for lithium-ion batteries. *Advanced Energy Materials*, *1*(6), 1079–1084.

Zhen, Z., & Zhu, H. (2018). Structure and Properties of Graphene. In *Graphene* (pp. 1–12). Elsevier.